International Journal for Multidisciplinary Research (IJFMR)
E-ISSN: 2582-2160 ● Website: www.ijfmr.com ● Email: editor@ijfmr.com

Computational Analysis of a Low Head Turbine with Cavitation Free Operation

Raji Rajan[1], Kishor K[2], Sajithgopi K V[3], Ampady O[4]

[1]Professor, Department of Mechanical Engineering, Aries Polytechnic College, Palakkad, Kerala, India
[2]H.O.S, Department of Mechanical Engineering, Aries Polytechnic College, Palakkad, Kerala, India
[3]Lecturer, Department of Mechanical Engineering, Aries Polytechnic College, Palakkad, Kerala, India
[4]Assistant Professor, Department of Mechanical Engineering, SNIT Adoor, Kerala, India

Abstract
A huge part of global population is using conventional energy, thereby consuming our future resources. In this scenario hydropower has come up as an attractive source of renewable energy because of its eco-friendly, pollution free nature and favorable future development. Low head micro hydropower station presents an attractive and efficient way for electricity generation in rural, remote and hilly areas because of the increment in the level of greenhouse gas emission and fuel prices in these sites and they have become increasingly popular for application of small rivers. The low head micro hydropower turbine is the most viable alternative solution to overcome the problem of lack of electric power supply and financial problems in rural and poor areas, in ensuring better future for the population. The research aims to design and analyze the performance of the turbine to evaluate influence of suction head by varying different vane parameters for the turbine and also takes a look into cavitation free operation in the path of the flow. The geometry modelling, mesh formation and simulation is done using Bladegen, Turbo grid and CFX respectively in ANSYS 19.0 version

Keywords: Low Head Turbine, ANSYS, Simulation, Performance, Modelling and Bladegen, Turbo grid and CFX

1. Introduction

Hydropower has been utilized for more than a hundred years, and it is the most efficient and confident source of renewable energy. Hydro-power contributes a large quantity of electricity for home, farm and plantation or for small village because water is a clear, cheap and eco-friendly source of energy generation. Low head micro-hydropower stations present a beautiful and efficient way for electricity generation. If enough water supplies are available, the low head micro-power system gives positive environmental impacts. Using low head hydro-power turbine, we can overcome the problems relating to the inaccessible sources of energy.

Using hydropower which is the largest source of renewable energy in the world will make noticeable impact in the field of power generation. The large scale and low head play an important role in the production of hydro-electric power. In hydroelectric power generation, large-scale centralized systems incur two problems: a decrease in suitable installation sites with high head, and the large environmental load associated with the civil engineering work. To overcome this defect, we can use small-head distributed types turbine. The small head turbines can be applied to low head systems such as pipelines,

small rivers and irrigation cannels etc. it is also required for civil works. So, the low head and micro-hydropower is the most secured alternative solution to overcome the problems of lack of electric power supply and financial problem in rural and poor areas, in ensuring better future for the population. These studies have focused on axial flow hydraulic turbines suitable for low head system. Conventional water turbines can be classified as impulse turbines or reaction turbines. The main types of conventional hydropower turbine types include Pelton turbines, Turgo turbines, cross-flow turbines, Francis turbines, Kaplan turbines, and tubular turbine.

The blade profile shown in Figure 1 is defined in terms of centerline (center surface) *f* and thickness function D distributed along the centerline. The centerline is obtained as the arithmetic mean of the pressure- and suction-side profiles of the aero foil. The thickness function depends on the distribution coefficient d. For thickness distribution coefficient δ =0, the centerline coincides with the suction-side profile, while for δ =1 the centerline coincides with the pressure-side of the aero foil. In general, there is no reason why δ =0 shouldn't exceed 1 or drop below 0. However, if this is allowed, the centerline will no longer be contained within the boundaries of the aero foil profile. Thus it is seen that the blade profile need to be defined like that of the aero foil.

Figure 1: Aero foil geometry

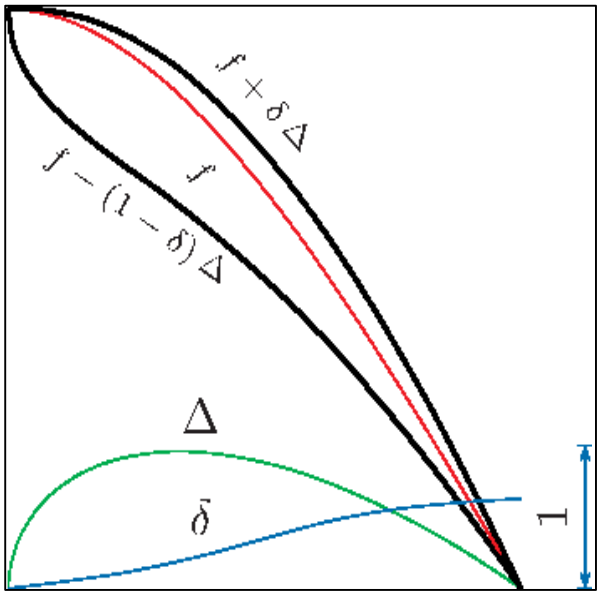

Y Nishi et.al (1), The study aims to redesign and optimize the existing runner to achieve more efficiency and more power. The study aims to redesign and optimize the existing runner to achieve more efficiency and more power. Loss rate of the guide vane was greater in optimized runner as compared to the original runner. The amount of vortices in the flow around optimized runner was lesser when compared that of original runner, because of that efficiency of the turbine increases.

S.F. Chini et.al (8), Developed a design model for very low head turbine runner blade. Developed a design model for very low head turbine runner blade. The design procedure was accomplished based on the classical free vortices theory at the runner section. They created turbine geometry by using blade gen and analysis is performed Ansys CFX 15 and governing equation are solved using the SST turbulence model to capture the turbulent structures. The maximum hydraulic efficiencies for many of the runner positions (at constant angular velocity of 40 rpm) are quite than 80%.

Jayson J. Martinez et.al (9), Design optimized composite runner blades for ultra-low head turbine. Replaced ordinary stainless steel blade with light weight composite blades compression molded from a fiber reinforced polymer. Compared composite turbine blade model with same stainless steel blade design. With the same flow rates, the composite turbine blades generated more power but required slightly higher head than the stainless steel blades. Both turbines showed similar peak turbine efficiency, demonstrating the potential of composite materials to replace SS as the turbine material from the perspective of power generation.

Abdul muis et.al (4), Conducted study on axial turbine for very low head application which operates on low speed. Design optimization is generated by optimizing the blade cascade development of the turbine blade. Blade airfoil is optimized to get optimum value of ratio of Lift coefficient Cl and Coefficient of drag Cd, within the range of turbine operation by utilizing of XFOIL that controlled via MATLAB. These airfoils are wont to develop the blade cascade. To increase the advantages of fluid flow passing through the turbine blades, the analysis and optimization of the blade cascade is conducted. Vortex panel method is employed to research the fluid flow inside cascade to realize the utmost of the lift force.

2. Objective

Primary objective of the project is to design ultra-low head turbine geometry for a power output of 500W and a head in the range of 5m to 10m. For a power output of 500W and head available in the range of 5 to 10 m, the installation of a Kaplan turbine is needed**.**

- To redesign the axial flow hydra turbine for cavitation free operation.
- To analyze the performance characteristics of the turbine by changing the mass flow rate and changing the speed of the turbine.
- To study the influence of tail rise height in the performance of the turbine.

3. Turbine Blade

The chord line may be a line connecting the leading and trailing edges of the airfoil. The chord is the length of the chord line from leading edge to trailing edge and is the characteristic longitudinal dimension of an airfoil. The mean camber line is a line drawn halfway between the upper and lower surfaces as shown in figure 2. The chord line connects the ends of the mean camber line. Maximum camber is the maximum distance between the mean camber line and the chord line. Maximum thickness refers to the utmost distance between the upper and lower surface. Leading edge radius is that the radius of curvature given the leading-edge shape.

Figure 2: Basic geometry of the blade profile

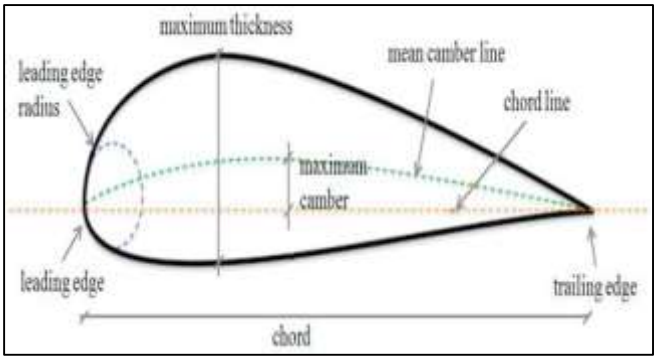

4. Parameters

4.1. Effect of Number of Blades

As the number of blades in the hydro turbine increases, it is seen that the vibration increases which simultaneously decreases the efficiency. As the number of blades increase, the blades should have a thin profile but blades with thin portion at the root may not withstand the stress induced due to axial load of the water flow throughout its work life. Therefore 4 blade systems with thick roots are preferred.

4.2. Blade Shape and Orientation

A turbine blade has airfoil cross-section from root to tip. The lift force generated when the wind flows over the airfoil is the driving force of the wind turbine. Lift force is perpendicular to the relative velocity and increases with the angle of attack. Though it also increases an undesirable drag force. Lift force supports the blade rotation while drag force opposes it. A turbine blade gives maximum performance when the lift to drag ratio is maximum which is achieved at the optimum angle of attack. For optimum angle of attack, the incoming stagnation streamline of flow must be in line with the chamber line of the blade profile. This would avert any shock wave that may lead to anything but smoothest entry along the turbine blade.

4.3. Hub to Tip Ratio

The ultra-low head turbines are preferred to have a hub to tip ratio of 0.3 to 0.5 for optimum performance of the turbine The flow in the blade rows of axial turbo machines with large hub to tip ratio can be approximated to the two-dimensional flow in a rectilinear cascade efficiency losses are generally reduced by,

- Avoiding low tip speed ratios which increase wake rotation
- Selecting airfoils which have a high lift to drag ratio
- Specialized tip geometries

4.4. Stagger Angle

The stagger angle is defined as the inclination of the chord line to the axis of rotation of the hub. The stagger angle may vary from 30º-70º. This inclination ensures the apparent blocking of water flow.

5. Cavitation

The formation, growth and collapse of vapour filled cavities or bubbles in a flowing liquid because of local fall in fluid pressure are called cavitation. When the pressure at any point during a flow field equals the vapour pressure of the liquid at that temperature vapour cavities (bubbles of vapour) begin to seem. It is presumed that a vapour cavity is made around dust nuclei which are within the liquid. The cavities thus formed, thanks to motion of liquid, are carried to high pressure regions where the vapour condenses and that they suddenly collapse. The adjoining liquid rushes with a very great velocity to occupy the empty spaces thus created, causes series of violent, irregular, spherical shock waves. When these irregular implosions occur on the metallic surfaces, they produce noise and vibration. When the cavities collapse on the surface of a body, due to repeated ‘hammering’ action, the metal particles give way ultimately due to fatigue and indentations are formed; this erosion of material is called pitting.

5.1. Cavitation in Hydraulic Machinery

Cavitation is the formation of the vapour bubbles in the liquid through any hydraulic turbine. In hydro turbines, dynamic pressure changes can occur, When the local pressure reduced to the vapor pressure cavities occurs and grows. Such a cavity consists of two phases, formation and growth. When the

pressure has increased this growing is reversed, and the bubble will collapse suddenly. The cavitating flow has the following effects on the hydraulic machines:

- Due to the low-pressure cavities that happen between the guide vane blades and the turbine runner, cross-sectional area decreased. According to the reduction of the cross-section area, discharge and power are reduced.
- When the bubbles are collapsed, turbine efficiency decreases to 10% to 20%.
- Cavitation erodes material surface. Those damaged surfaces expand due to continuous cavitation. With the increase of the erosion, material particles detach from the surface.
- Unstable radial hydraulic forces which are results of the cavitation, effects turbine rotor and turbine generator shaft. Those unstable forces create vibration and oscillation, which decreases the efficiency of the hydraulic bearings of the generator.

6. Simulation Modelling

The simulation is done on a model of axial turbine. The model of the turbine is modeled to scale for simulation in Bladegen, followed by meshing in the Turbogrid and analysis is done over CFX fluent in the Ansys 19.0 version.

6.1. Geometry Design

The turbine test section is designed based on the parameter like power output and the head while assuming certain parameters like discharge and geometric features based on literature review. Following parameters were therefore taken into consideration while designing the turbine geometry in Bladegen component systems in ANSYS software version 19.0

No of blades = 4
Hub to tip ratio = 0.35
Hub diameter = 65 mm
Blade diameter =185 mm

Figure 3: Model create in Bladegen

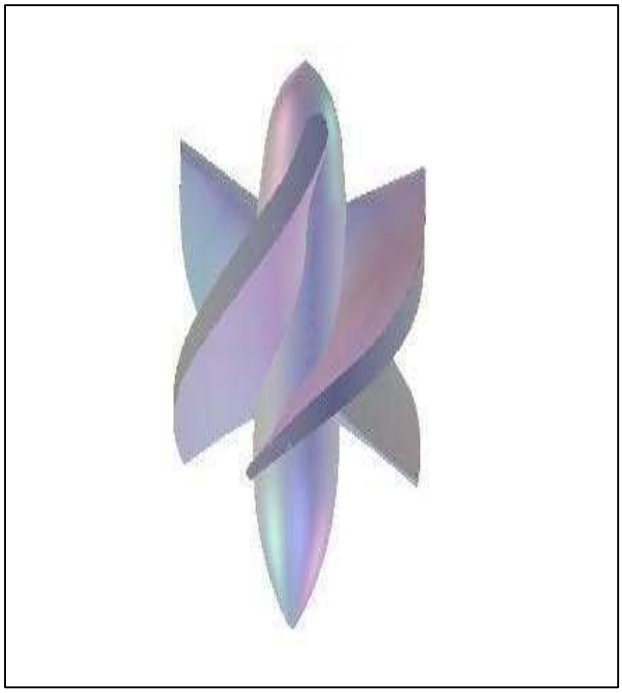

6.2. Mesh generation

The turbine geometry data was then transferred to the Turbo grid component systems in the ANSYS software for mesh generation as shown in fig 4. The mesh is initially maintained at a global default size factor of 1.5. The mesh is then modified by hit and trial method until the simulation setup brings a mesh conditions that converges. It is observed that the simulation setup converges when the inlet and outlet passage are assigned with H-grid structure with the grid size factor as 1.1 at inlet and 1.2 at the outlet. The passage is then maintained at a grid factor of 1.5. No of nodes is 152675 and No of elements =13932.

Figure 4: Mesh generation in the geometry

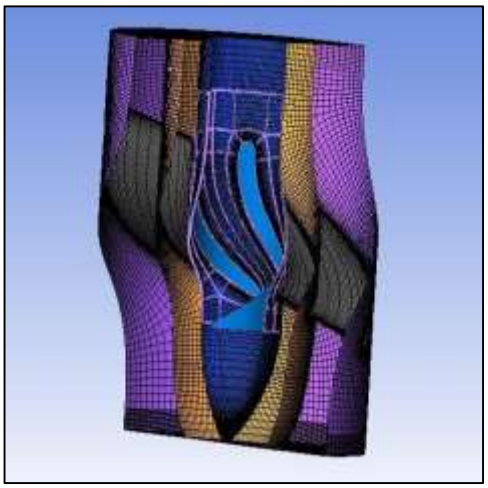

6.3. Simulation

The turbine geometry is simulated in CFX in ANSYS 19.0 software. During the simulation, the water enters the turbine test section as a non-buoyant continuous fluid as shown in figure 5. The mass flow rate at inlet is 5 kg/sec while the rotor turns at 1500rpm and output pressure is 1atm. K-e turbulence model is taken for simulation based on literature review. The set of equation working parallel while the geometry undergoes simulation are Continuity equation, Reynolds equation, Equation for turbulent viscosity m*t* and 2 equations from k-e model (transport of kinetic energy of velocity fluctuations k and transport of kinetic energy of velocity fluctuations e)

Figure 5: simulation condition setup

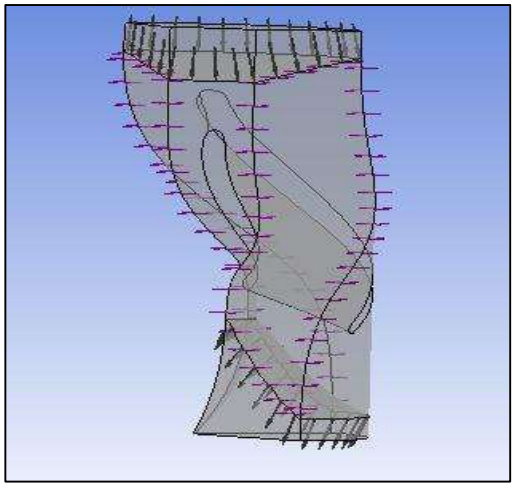

7. Governing Equations

Based on the above assumptions, the governing equations for mass and momentum for a steady three-dimensional flow in the fluid domain and the energy equation in the solid region are as follows:

7.1. Conservation of Mass

The equation for conservation of mass is:

$$\left(\frac{\partial u}{\partial t}\right) + \left(\frac{\partial v}{\partial t}\right) + \left(\frac{\partial w}{\partial t}\right) = 0$$

7.2. Conservation of momentum

X- Momentum equation:

$$u\left(\frac{\partial u}{\partial x}\right) + v\left(\frac{\partial u}{\partial y}\right) + w\left(\frac{\partial u}{\partial z}\right) = \nu\left[\left(\frac{\partial^2 u}{\partial x^2}\right) + \left(\frac{\partial^2 u}{\partial y^2}\right) + \left(\frac{\partial^2 u}{\partial z^2}\right)\right] - \left(\frac{1}{\rho}\right)\left(\frac{\partial P}{\partial x}\right)$$

Y- Momentum equation:

$$u\left(\frac{\partial v}{\partial x}\right) + v\left(\frac{\partial v}{\partial y}\right) + w\left(\frac{\partial v}{\partial z}\right) = \nu\left[\left(\frac{\partial^2 v}{\partial x^2}\right) + \left(\frac{\partial^2 v}{\partial y^2}\right) + \left(\frac{\partial^2 v}{\partial z^2}\right)\right] - \left(\frac{1}{\rho}\right)\left(\frac{\partial P}{\partial y}\right)$$

Z- Momentum equation:

$$u\left(\frac{\partial w}{\partial x}\right) + v\left(\frac{\partial w}{\partial y}\right) + w\left(\frac{\partial w}{\partial z}\right) = \nu\left[\left(\frac{\partial^2 w}{\partial x^2}\right) + \left(\frac{\partial^2 w}{\partial y^2}\right) + \left(\frac{\partial^2 w}{\partial z^2}\right)\right] - \left(\frac{1}{\rho}\right)\left(\frac{\partial P}{\partial z}\right)$$

7.3. SST model

The governing of the simulation study is done based on the shear-stress transport (SST) equations. The shear-stress transport (SST) k-ω model was developed by Menter to effectively blend the robust and accurate formulation of the k-ω model in the near-wall region with the free-stream independence of the k-e model within the far field. To achieve this, the k- e model is converted into a k-ω formulation. Transport Equations for the SST k-ω Model:

$$\frac{\partial(\rho k)}{\partial t} + \frac{\partial(\rho k u_i)}{\partial x_i} = \frac{\partial}{\partial x_j}\left[\left(\Gamma_k \frac{\partial k}{\partial x_j}\right)\right] + G_k - Y_k + S_k$$

and

$$\frac{\partial(\rho\omega)}{\partial t} + \frac{\partial(\rho\omega u_i)}{\partial x_i} = \frac{\partial}{\partial x_j}\left[\left(\Gamma\omega \frac{\partial \omega}{\partial x_j}\right)\right] + G\omega - Y\omega + D\omega + S\omega$$

7.4. Boundary conditions

There are 5 boundaries created in the rotor model:

1. R1 Blade: It is maintained as wall with free slip condition

2. R1 Hub: The hub in block, out block and passage is assigned free slip wall condition.
3. R1 Inlet: the in block inflow is assigned mass flow rate depending upon individual cases run in direction normal to the boundary.
4. R1 Outlet: the out block outflow boundary is assigned average static pressure of 1 atm.
5. R1 Shroud: In block shroud, out block shroud, passage shroud is assigned the free slip wall.

8. Results

The simulation analysis on the performance of the rotor model is summarized. Based on the variation of the mass flow rate and the rotational speed of the turbine, the following details were gathered. The simulation is done over Ansys 19.0 where SST turbulence model is used. In the simulation it is assumed that the mass flow of water through the turbine section is uniform and steady i.e. it shows full-fledged water flow through the turbine section. Based on the simulation, following contours of velocity and pressure and also graphs of torque output, power output, pressure drop, efficiency, torque coefficient, power coefficient and minimum pressure condition at outlet were created with respect to variation of rotational speed for the varying mass flow rates.

8.1. Torque vs. Rotational Speed

It is observed that the torque increases with increase in mass flow rate and the rotational speed of the turbine. From the graph, it can be seen that the max torque output is for the mass flow rate of 20kg/sec at 1800rpm. But the most optimum steady output is seen for the mass flow rate of 18kg/sec for rotational speed of 1500 rpm and above.

Figure 6: Torque vs. rotational speed

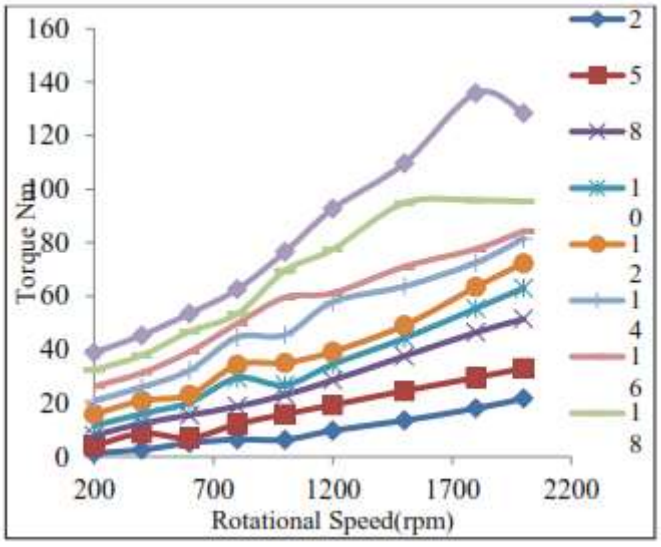

8.2. Efficiency vs. Mass Flow Rate

It is observed from Figure 7 that the efficiency of the water flow through the passage of the rotor model is increasing with the increase in the mass flow rate and the rotational speed of the model. The power output of the turbine section is seen to be high for corresponding mass flow rate and rotational speed of the turbine. The efficiency is observed to be the maximum at 75.54% for the mass flow rate of 10kg/sec and 1200rpm. With increase in the mass flow rate and the rotational speed the efficiency increases until the optimal efficiencies for individual mass flow rates are achieved

Figure 7: Efficiency vs. Mass Flow Rate

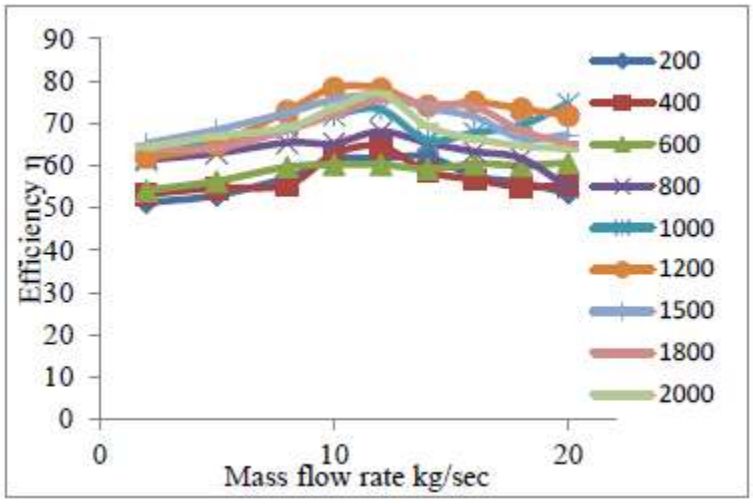

8.3. Pressure contour

The simulation is done in a steady state where mass flow input is 5kg/sec in the standard conditions with no heat. It is seen that the pressure through the test decreases in the downward direction as shown in fig 8. A negative value of pressure is seen due to the absence of the draft tube. The presence of draft tube as a diverging path will prevent the pressure from reaching a negative value and also the chances of creating suction

Figure 8: Pressure contour in the test section

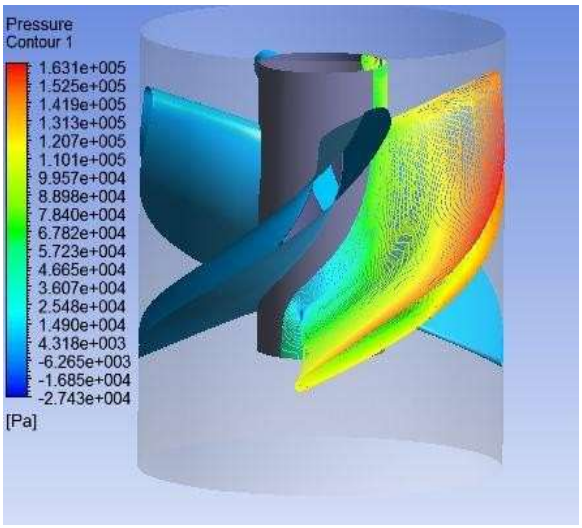

8.4. Velocity contour

It is observed that the velocity increases as the water passes through the test section as shown in fig 9. As the water flows by the walls of the hub, the velocity is zero due to no slip condition. The water flows along the pressure side of the blade profile and detaches towards the suction side of the blade prior to the blade it is flowing over. As a result, the velocity contour shows a higher velocity on the suction side of the blade profile in the turbine.

Figure 9: Velocity contour in the test section.

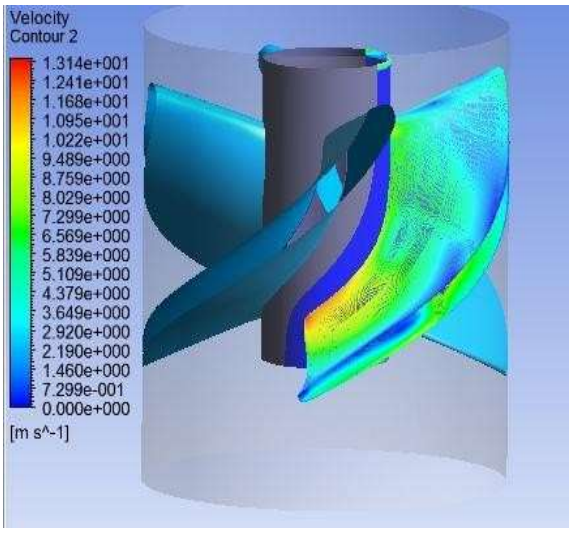

8.5. Cavitation

The graph in Figure 10 shows the pressure condition of the water at turbine outlet. It shows that the pressure conditions at the outlet of the turbine are higher than the vacuum pressure in normal atmospheric condition. Thus there is no possibility of the occurrence of cavitation in the rotor model.

Figure 10: Minimum pressure output in each case of mass flow rate.

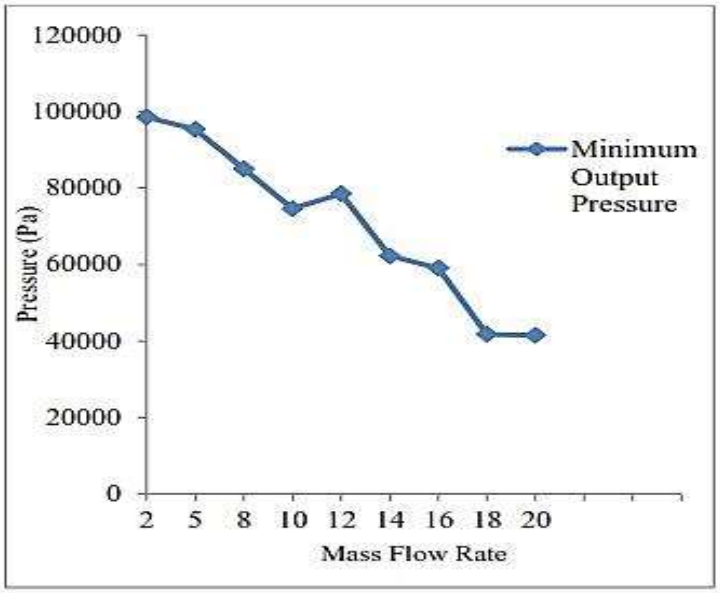

9. Calculations

It is seen that the force in the test section is 28.56 N. Therefore, the torque and power can be calculated as follows. Torque = Force * displacement Nm and

Power = $\frac{2\pi NT}{60}$ W

Therefore, the torque received at the end of the turbine is 2.32 Nm and the power measured is 364.24W.

10. Conclusions

The results indicate that the torque of the turbine increases with an increase in mass flow rate and rotational speed. Similarly, the efficiency of water flow through the rotor passage improves with higher mass flow rates and rotational speeds, leading to an increase in the power output of the turbine. The pressure at the turbine outlet is observed to be higher than the vacuum pressure under normal atmospheric conditions, which confirms that there is no possibility of cavitation in the rotor model. However, the pressure contour exhibits negative values, suggesting the necessity of incorporating a draft tube for efficient operation. The velocity is found to be higher on the suction side of the blade profile due to the interaction of water flow along the blade surface. The turbine produces a torque of **2.32 Nm** with a corresponding power output of **364.24 W**.

11. References

1. Yasuyuki Nishi , Tomoyuki Kobori (2019) 'Study of the internal flow structure of an ultra-small axial flow hydraulic turbine'
2. Swe Le Minn et al. (2014) 'Design and Vibration Characteristic Analysis of 10kW Kaplan Turbine Runner Blade Profile.'
3. Abdul Muis et al. hoen (2015) 'Design optimization of axial hydraulic turbine for very low head application.' Sustainable Energy Engineering, pp. 263-273.
4. Marzena Banaszek and Krzyztof Tesch (2010) 'Rotor blade geometry optimization in Kaplan turbine.'
5. C.P Jawahar et al. (2017) 'A review on turbines for micro hydro power plant', Renewable and Sustainable Energy Reviews, Vol 72, 882–887.
6. Donna Frunza Verde et al. (2016) 'Failure analysis of a Kaplan turbine runner blade by metallographic and numerical method.'
7. Norio Kikuchi et al. (2016) 'The Design Method of Axial Flow Runners Focusing on Axial Flow Velocity Uniformization', International Journal of Rotating Machinery Vol 216, pp. 113-126.
8. S.F. Chini, et al. (2018) 'Developing a method to design and simulation of a very low head axial turbine with adjustable rotor blades',
9. Jayson J. Martinez et al. (2018) 'Design and Performance of Composite Runner Blades for Ultra Low Head Turbines', Renewable Energy pp. 1481-1492.
10. Pankaj P. Amonkar et al. (2016) 'Structural Analysis on Micro-Hydro Kaplan Turbine Blade', International Journal for Innovative Research in Science & Technology vol. 2 pp. 12-26.
11. Mr. L. Srinivas Naik et al. (2017) 'Design and Analysis of Low Head, Light weight Kaplan Turbine Blade', International Refereed Journal of Engineering and Science vol.2 pp. 17-2